Electronic Supplementary Material (ESI) for Soft Matter.

Supporting Information: Microscopically segregated ligand distribution in co-assembled peptide-amphiphile nanofibers

Turash Haque Pial,[a,b] Yang Li,[b,c] Monica Olvera de la Cruz*[,a,b,c,d,e]

[d]Department of Materials Science and Engineering, Northwestern University, 2220 Campus Drive, Evanston, IL 60208, United States

[b]Center of Computation and Theory of Soft Materials, Northwestern University, 2145 Sheridan Road, Evanston, IL 60208, United States

[c]Department of Chemical and Biological Engineering, Northwestern University, 2145 Sheridan Road, Evanston, IL 60208, United States

[d]Department of Physics and Astronomy, Northwestern University, 2145 Sheridan Road, Evanston, IL 60208, United States

[e]Department of Chemistry, Northwestern University, 2145 Sheridan Road, Evanston, IL 60208, United States

* Email: m-olvera@northwestern.edu

S.1: Simulation details:

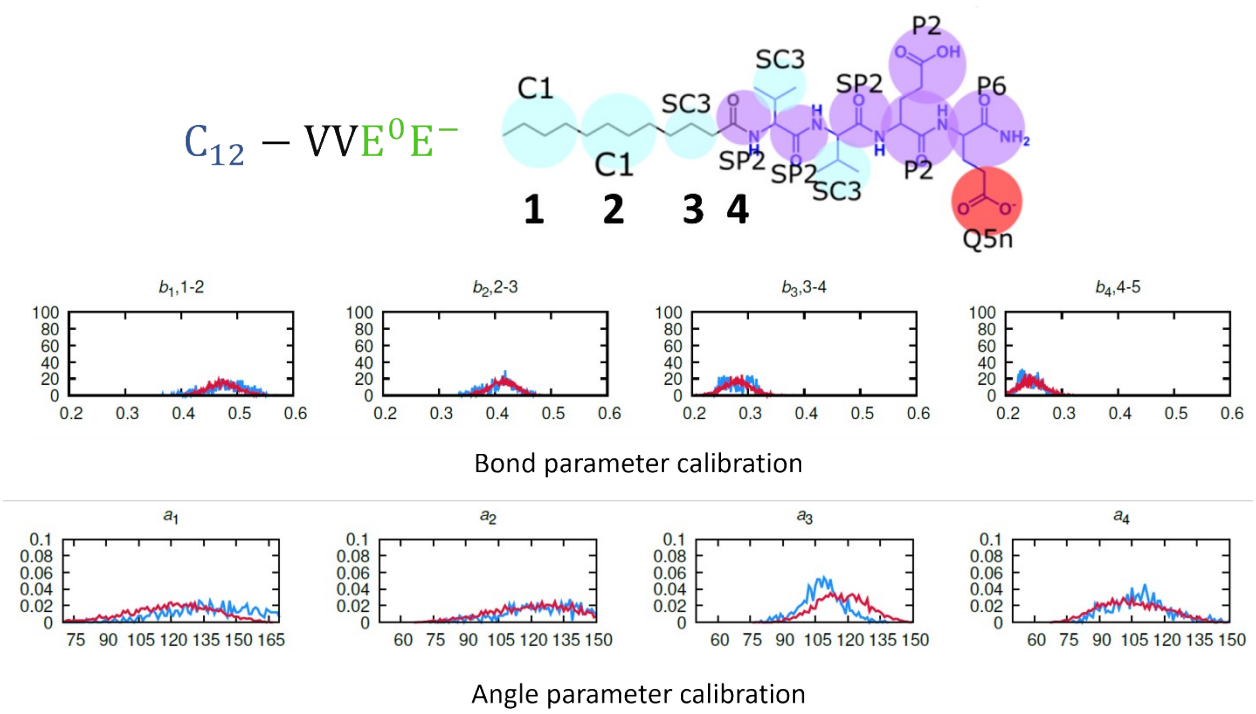

Figure S1. Definition of Martini3 beads of $C_{12}VVEE$ *and parameter calibrations.*

As non-amino acid parameters are not provided by martini3 [1] or martinize2 [2], we followed the small molecule modeling techniques for bead definitions [3]. As bond angle parameters are not provided for C12, we have performed simulations to iteratively adjust the bond distance, bond strength, angle, and angle strength by following this tutorial [4]. In Figure S1, we are showing the bond and angle distribution where the blue curves show the all-atom distribution and red curve show our coarse-grain distribution. Our surface accessible surface area was also in between 8% of the all-atom value.

Z33 is made of 33 amino acids which forms a double alpha helix structure. We used martinize2 [2] to directly get bead definitions, bond, angle, dihedral and constrain parameters. All-atom to Martini3 mapping is shown in Figure S2. The chemical structure and single letter description of Z33 is also shown. The hydrophobic amino acids are indicated with green letters.

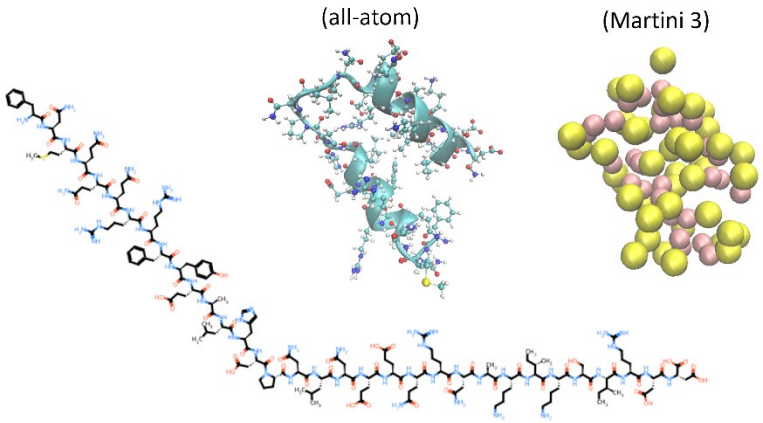

Figure S2. Definition of Z33 and its chemical structure. All-atom and Martini 3 depiction of Z33 is also shown.

In Martini3 simulations, the potential energy was first minimized using the steepest descent algorithm for 5000 steps. An NVT ensemble equilibration was performed for 1000 steps with a timestep of 10 fs. The v-rescale thermostat was utilized to keep the temperature constant. Subsequently, an NPT ensemble equilibration was carried out for 1000 steps with a timestep of 10 fs. The v-rescale thermostat and Berendsen barostat were utilized. Finally, a long MD production run was performed with a timestep of 20 fs until the co-assembly process is finished. Neighbor searching was performed up to a cut-off distance of 1.2 nm by means of the Verlet particle-based approach and was updated every 20 timesteps. The potential-shift method was applied for the short-range Lennard-Jones (LJ) 12-6 interactions at a cut-off of 1.2nm. The Particle Mesh Ewald method was used for calculations of the non-bonded interactions between charge beads (cut-off 1.2 nm). The dielectric constant was fixed at 15. The bonds were constrained with the LINCS algorithm. The temperature of the PAs and solvent/ion molecules were separately coupled using the v-rescale algorithm (reference temperature 298 K, characteristic time 1 ps). The isotropic Parrinello-Rahman barostat was utilized with the reference pressure of 1 bar, the characteristic time of 12 ps, and the compressibility of 4.5 × 10-4 bar-1 in all directions. After initial co-assembly, isotropic barostat is changed into semi-isotropic along the fiber axial direction. Periodic boundary conditions were applied in all three dimensions.

We run simulations for 10μs after the co-assembly process is completed and analyzed last 3μs data. As Martini3 is not an all-atom model, the dynamics is fast, so we are assuming we have performed enough production run. We have also checked how the number-average cluster size changed with time for the simulation with a ligand-filler ratio of 1/5 (no salt), as this should be most crowded. The number-average cluster size is defined as $CSN = \frac{\sum N * M}{\sum M}$, where N is the cluster size and M is the concentration of the cluster. We can see from Figure S3, CSN reduces quickly in few hundred ns, probably breaking up micelles which were created during the co-assembly process.

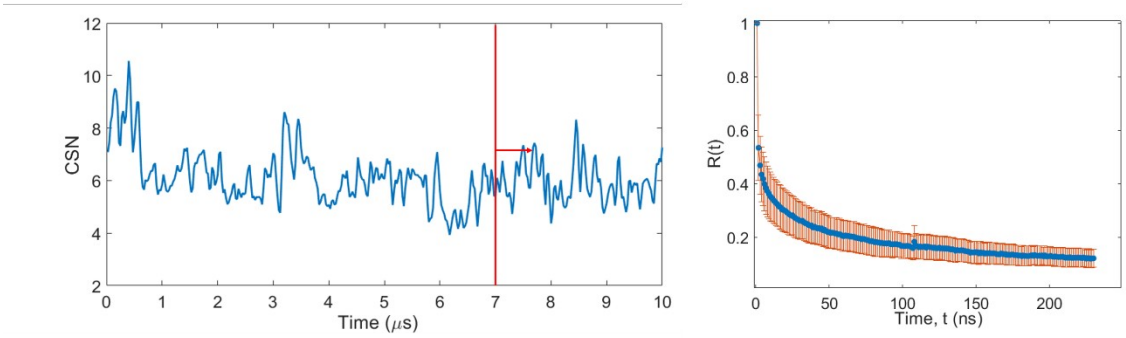

Figure S3. (left) CSN variation with time for the simulation of a ligand-filler ratio of 1/5, with no salt. (right) Residence time correlation function for the equilibrated system.

To check if the system is equilibrated and peptides are not stuck in a local minimum, we have calculated the residence time correlation function for inner Valine (SP2 bead) of simulations with ligand-filler ratio of 1/5 (no salt). The residence time correlation function $[R(t)]$ is defined as

$$R(t) = \frac{1}{N}\sum_{i=1}^{N}\theta_i(t_0)\theta_i(t_0 + t)$$

Here θ_i is the Heaviside unit step function (if one Valine SP2 bead i resides inside the first solvation shell of another Valine SP2 bead, θ_i = 1; otherwise, θ_i= 0), N is the number of SP2 beads in the first solvation shell and t_0 is the initial time step. We used the inner Valine as it should be the least mobile among other peptide groups. This residence time is averaged for all beads and over 50 different initial time steps after equilibration. Error bar is obtained from 3 different simulations. $R(t)$ indicates how long the beads stay together. A larger $R(t)$ with time indicates that beads are hardly diffusing and probably stuck in a local environment. For our case, we can see that $R(t)$ values go below $1/e$ in few nanoseconds, which indicates

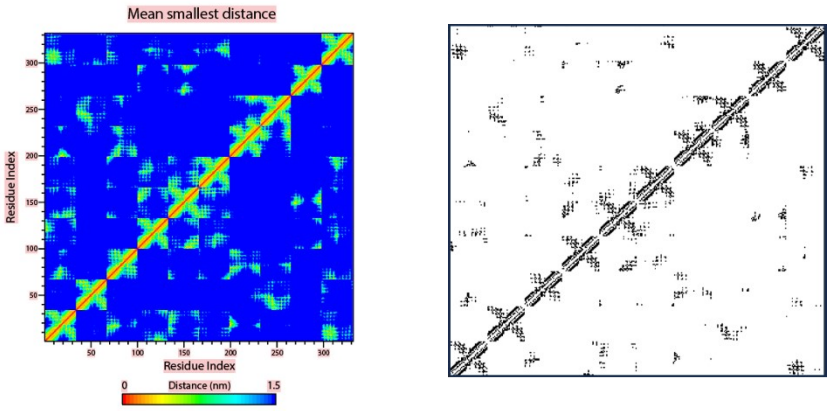

Figure S4. A visual representation of the contact map matrix for 10 amino acids in all-atom simulation. Both shows the same matrix values but with different color scheme. Different color represents different minimum distance among amino acid residues.

that our peptides in the fiber are vary mobile and not stuck in a local minimum. This also says that our production period of 3 μs is more than enough to sampling the equilibrated system.

We have performed the martini bulk simulation for 5μs after the initial formation of large aggregates and the full 5μs data was used as production run. All the simulation procedures remain same for Martini3 case. For all-atom, the potential energy was first minimized using the steepest descent algorithm for 10000 steps with a time step of 1 fs and a tolerance of 1000 N. A subsequent NVT ensemble equilibration of 1 ps was performed. Then, the NPT ensemble was applied for 4 sequent equilibrations of 5 ns each using the time step of 2 fs. For each NPT ensemble equilibration, the position restraint force constant decreases (1000 kJ/mol, 600 kJ/mol, 300 kJ/mol, and 0) to fully relax the structure. The pressure was coupled isotopically. Periodic boundary conditions were applied in all three dimensions. Neighbor searching was performed up to a cut-off distance of 1.2 nm by means of the Verlet particle-based approach and was updated every 20 timesteps. The potential-switch method was applied for the short-range Lennard-Jones (LJ) 12-6 interactions from 1 nm to 1.2 nm. The short-range electrostatic interactions were calculated up to 1.2 nm, and the long-range electrostatic interactions were calculated by means of the Particle Mesh Ewald algorithm. A time step of 2.5 fs was employed by constraining all the covalent bonds in amino acid using the LINCS algorithm. We have performed the production period for 2μs in all-atom simulations after initial aggregate formation.

We have used VMD contact map plugin to calculate nearest neighbor number. This analysis provides a contact map for all the amino acids present in the simulation system. In Figure S4, we are showing a graphical representation of the contact map matrix for all-atom bulk simulation, no salt case. This matrix provides the shortest distance between all amino acid residues, and we have used a cut-off 0.7 nm to calculate the nearest neighbor.

S.2. Co-assembly of similarly charged ligands and fillers.

Figure S5(a) shows the destabilized region in the fiber with negatively charged fillers and negatively charged ligands. We did not observe a breakout of micelles from the fiber during our total simulation time. In Figure S5(b), we show the difference between positive (upper panel) and negative (lower panel) ligands co-assembling into an already formed fiber of negative fillers. It is obvious from the snapshots that, all the positive ligands enter the fiber in 1μs. But only a fraction of negative ligands enters the fiber.

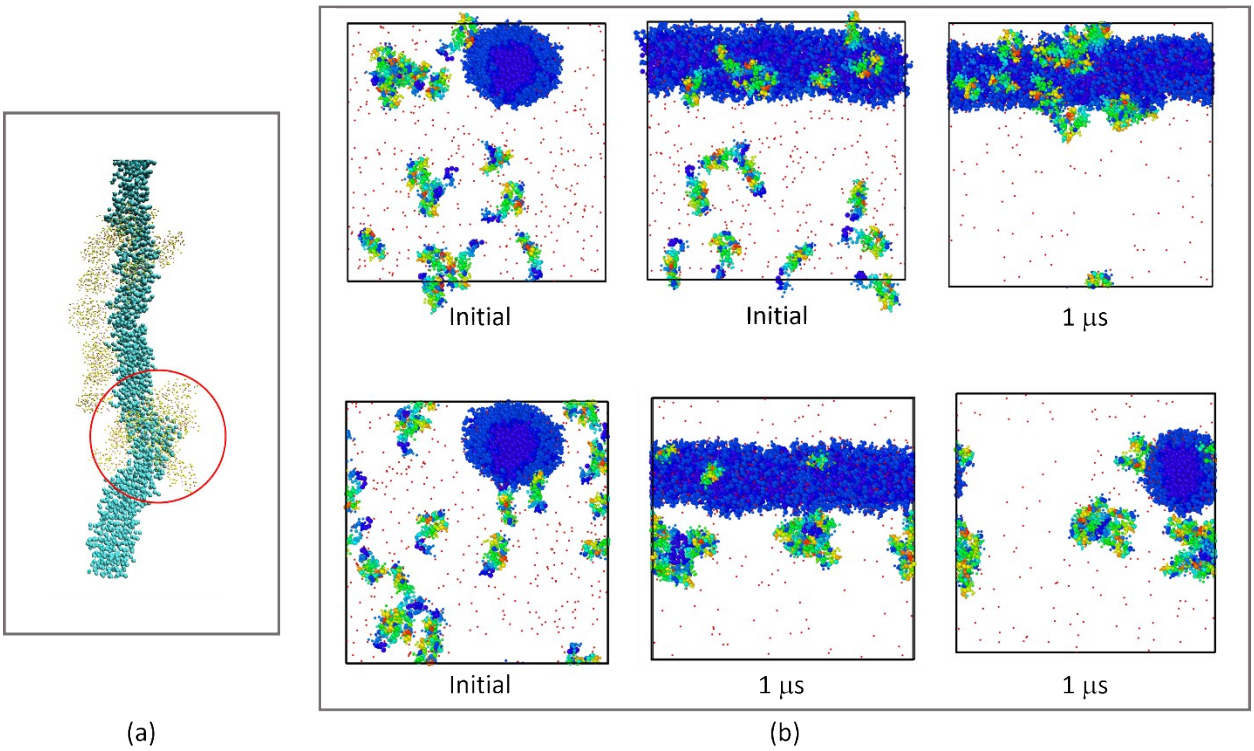

Figure S5. (a) A destabilized region in fiber where negative ligands are crowding. (b) Initial and final snapshots of the simulation systems where we tried to observe how many of the positively charged (upper panel) and negative charged (lower panel) enter a negatively charged fiber.

References:

[1] Souza, P. C. T.; Alessandri, R.; Barnoud, J.; Thallmair, S.; Faustino, I.; Grünewald, F.; Patmanidis, I.; Abdizadeh, H.; Bruininks, B. M. H.; Wassenaar, T. A.; Kroon, P. C.; Melcr, J.; Nieto, V.; Corradi, V.; Khan, H. M.; Domański, J.; Javanainen, M.; Martinez-Seara, H.; Reuter, N.; Best, R. B.; Vattulainen, I.; Monticelli, L.; Periole, X.; Tieleman, D. P.; de Vries, A. H.; Marrink, S. J. Martini 3: A General Purpose Force Field for Coarse-Grained Molecular Dynamics. Nat. Methods 2021, 18 (4), 382–388.

[2] Kroon, P C; Grunewald, F.; Barnoud, J; van Tilburg, M.; Souza, P C T.; Wassenaar, T A.; Marrink, S J.; Martinize2 and Vermouth: Unified Framework for Topology Generation. arXiv: 2212.01191, 2022

[3] Alessandri, R.; Barnoud, J.; Gertsen, A. S.; Patmanidis, I.; deVries, A. H.; Souza, P. C. T.; Marrink, S. J. Martini 3 Coarse-Grained Force Field: Small Molecules, *Adv. Theory Simul.* **2022**, *5*, 2100391

[4] http://cgmartini.nl/index.php/martini-3-tutorials/parameterizing-a-new-small-molecule